JACS
JOURNAL OF THE AMERICAN CHEMICAL SOCIETY
Article
pubs.acs.org/JACS

# Probing the 5f Orbital Contribution to the Bonding in a U(V) Ketimide Complex

Lani A. Seaman,[†] Guang Wu,[†] Norman Edelstein,*[,‡] Wayne W. Lukens,*[,‡] Nicola Magnani,[‡] and Trevor W. Hayton*[,†]

[†]Department of Chemistry and Biochemistry, University of California, Santa Barbara, California 93106, United States
[‡]Chemical Sciences Division, Lawrence Berkeley National Laboratory, Berkeley, California 94720, United States

Supporting Information

**ABSTRACT:** Reaction of $UCl_4$ with 5 equiv of Li(N=C$^t$BuPh) generates the homoleptic U(IV) ketimide complex [Li(THF)$_2$][U(N=C$^t$BuPh)$_5$] (**1**) in 71% yield. Similarly, reaction of $UCl_4$ with 5 equiv of Li(N=C$^t$Bu$_2$) affords [Li(THF)][U(N=C$^t$Bu$_2$)$_5$] (**2**) in 67% yield. Oxidation of **2** with 0.5 equiv of $I_2$ results in the formation of the neutral U(V) complex U(N=C$^t$Bu$_2$)$_5$ (**3**). In contrast, oxidation of **1** with 0.5 equiv of $I_2$, followed by addition of 1 equiv of Li(N=C$^t$BuPh), generates the octahedral U(V) ketimide complex [Li][U(N=C$^t$BuPh)$_6$] (**4**) in 68% yield. Complex **4** can be further oxidized to the U(VI) ketimide complex U(N=C$^t$BuPh)$_6$ (**5**). Complexes **1**−**5** were characterized by X-ray crystallography, while SQUID magnetometry, EPR spectroscopy, and UV−vis−NIR spectroscopy measurements were also preformed on complex **4**. Using this data, the crystal field splitting parameters of the f orbitals were determined, allowing us to estimate the amount of f orbital participation in the bonding of **4**.

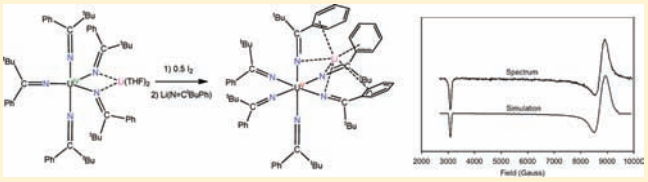


## INTRODUCTION

Interest in understanding the extent of covalency in actinide−ligand bonding has grown substantially in recent years.[1−13] This interest is motivated, in part, by the need for new extractants in advanced nuclear fuel cycles.[8−10,14] A variety of experimental techniques have been used to quantify covalency in these elements,[1,15−17] including ligand K-edge X-ray absorption spectroscopy,[4,18] photoelectron spectroscopy,[19] EXAFS,[11,20] X-ray crystallography,[21−28] and thermochemistry.[22,29] Optical spectroscopy can also provide useful information on bonding in the actinides. For instance, using NIR spectral data, Edelstein and co-workers were able to extract the $\theta$, $\Delta$, and $\xi$ ligand field parameters for a series of homoleptic 5f$^1$ actinide halides.[30,31] They suggested that the presence of covalency in the An-X $\sigma$-bonding framework best explained the observed trends in these parameters. Unfortunately, this analysis was limited by the paucity of complexes with both octahedral symmetry and the correct electronic configuration. For this technique to be applied more broadly, the synthesis of new, high symmetry 5f$^1$ complexes is required. In this context, our research group has demonstrated that high valent, octahedral alkoxide, amide, and alkyl complexes of uranium are, in fact, readily isolable.[32−35]

In our continuing efforts to synthesize homoleptic complexes of uranium in the 5+ and 6+ oxidation states, we have turned our attention to the ketimide ligand, in particular [N=C$^t$BuPh]$^-$ and [N=C$^t$Bu$_2$]$^-$. Recent studies by our group have shown that ketimides are capable of supporting high oxidation states, such as the strongly oxidizing Mn(IV) and Fe(IV) ions.[36,37] This stabilization likely arises from a combination of the ketimide's strong $\sigma$-donating ability (the p$K_a$ of Ph$_2$C=NH is 31)[38] and its strong $\pi$-donating ability.[37,39] Moreover, ketimides are noted for being inert coligands that do not exhibit insertion chemistry[39−42] and which are resistant to electrophilic attack,[41] making them good ligands for the exploration of small molecule chemistry. Ketimides are also easily synthesized[43] and are highly tunable.[44−46]

Kiplinger and co-workers have synthesized an expansive series of actinide ketimides with the general formula of Cp*$_2$An(N=CR$_2$)$_2$ (An = Th, U; R = alkyl, aryl).[47−57] Theoretical calculations and spectroscopic analysis of this series of complexes suggests that ketimides exhibit relatively covalent metal−ligand interactions, due, in part, to their significant $\pi$-donating capability.[37,39] Further insight into the metal−ketimide interaction comes from an electrochemical study of a series of U(V) imido complexes, Cp*$_2$U(NAr)X (Ar = 2,6-$^i$Pr$_2$C$_6$H$_3$; X = OTf, I, Cl, Br, SPh, F, Me, OPh, N=CPh$_2$). For this series, the ketimido derivative exhibited the lowest U(VI)/U(V) redox potential,[49] further demonstrating the strong electron donating ability of this ligand class. In addition to the work of Kiplinger, Cummins and Diaconescu reported the synthesis of a U(III) inverted arene sandwich complex, K$_2$($\mu$-$\eta^6$,$\eta^6$-C$_{10}$H$_8$)[U(NC[$^t$Bu]Mes)$_3$]$_2$,[58] demonstrating that ketimides can also stabilize the 3+ state of uranium.

Herein we report the synthesis of a series of homoleptic uranium ketimides in the 4+, 5+, and 6+ oxidation states. In addition, we present a detailed spectroscopic analysis of an octahedral U(V) ketimide, allowing us to estimate the amount of f orbital participation in the uranium−ketimide interaction.

**Received:** December 20, 2011
**Published:** February 10, 2012

## RESULTS AND DISCUSSION

**Synthesis.** Addition of 5 equiv of Li(N=C$^t$BuPh) to $UCl_4$ in THF results in the formation of a dark brown solution, from which $[Li(THF)_2][U(N{=}C^tBuPh)_5]$ (**1**) can be isolated as a brown solid in 71% yield by crystallization from concentrated hexanes (eq 1). Similarly, addition of 5 equiv of Li(N=C$^t$Bu$_2$)

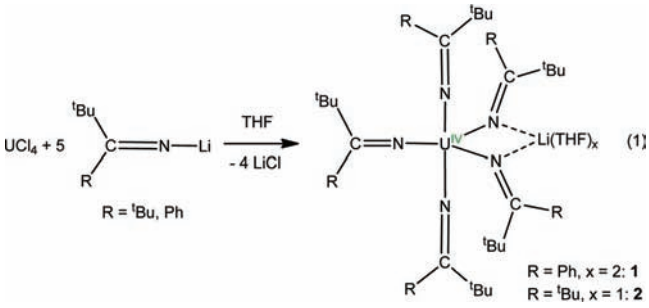


to $UCl_4$ provides the homoleptic uranium(IV) ketimide, $[Li(THF)][U(N{=}C^tBu_2)_5]$ (**2**), which is isolable in 67% yield after crystallization from hexanes (eq 1).

Complex **1** is soluble in both nonpolar and ethereal solvents. Its $^1$H NMR spectrum in $C_6D_6$ displays resonances at 12.33, 7.73, and 7.43 ppm in an 2:1:2 ratio. These resonances are attributable to the *ortho*, *para*, and *meta* protons on the phenyl rings, respectively. A resonance at −5.01 ppm can be assigned to the *tert*-butyl protons, while the resonances of the THF molecules are observed at 0.28 and 1.35 ppm. Additionally, **1** exhibits a single resonance in the $^7$Li NMR spectrum at 14.52 ppm. Complex **2** is also highly soluble in hexanes, toluene, and ethereal solvents. Its $^1$H NMR spectrum in $C_6D_6$ exhibits resonances at 4.24, 1.56, and −1.47 ppm, corresponding to the $\alpha$-THF protons, the $\beta$-THF protons, and the *tert*-butyl protons, respectively. Its $^7$Li NMR spectrum exhibits a single resonance at 89.38 ppm.

Storage of a concentrated hexanes solution of **1** at −25 °C affords crystals suitable for X-ray analysis. Complex **1** crystallizes in the triclinic space group $P\bar{1}$, and its solid state molecular structure is shown in Figure 1. In the solid state, **1** adopts a trigonal bipyramidal geometry. The U−N bond lengths for the terminal ketimide ligands range from 2.248(4) to 2.260(4) Å, whereas the U−N bond lengths of the bridging ketimide ligands are 2.313(4) and 2.335(3) Å. The U−N bond lengths are within the range of U(IV) amide complexes.[32,59] They are also in the range of other uranium ketimide U−N distances (2.176(12)−2.343(7) Å).[49,58] The terminal ketimide U−N−C bond angles are nearly linear, ranging from 170.9(4)° to 173.4(5)°, consistent with an sp hybridized nitrogen participating in $\pi$-donation to the uranium metal center. However, given the steric bulk of the ketimide ligand, it is possible that the large U−N−C angles are a result of steric crowding. Finally, the lithium cation in **1** is ligated by two THF molecules and two nitrogen atoms from the ketimide ligands, giving the lithium a tetrahedral geometry. Complex **2** also exhibits a trigonal bipyramidal geometry around the uranium center (see the Supporting Information), with similar metrical parameters. As with **1**, the lithium cation in **2** is contained within the secondary coordination sphere; however, its coordination environment consists of two ketimide nitrogen atoms, one THF molecule, and agostic interactions with the ketimide methyl groups.[36,37]

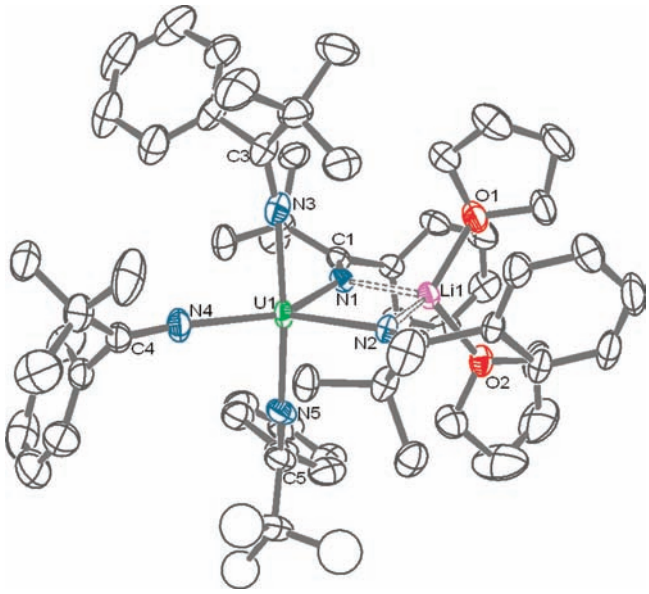


**Figure 1.** ORTEP diagram of $[Li(THF)_2][U(N{=}C^tBuPh)_5]$ (**1**) with 50% probability ellipsoids. Selected bond lengths (Å) and angles (deg): U1−N1 = 2.313(4), U1−N2 = 2.335(3), U1−N3 = 2.248(4), U1−N4 = 2.260(4), U1−N5 = 2.251(5), C1−N1−U1 = 145.7(3), C2−N2−U1 = 143.6(3), C3−N3−U1 = 170.9(4), C4−N4−U1 = 173.4(5), C5−N5−U1 = 172.2(4).

Interestingly, addition of 6 equiv of either Li(N=C$^t$BuPh) or Li(N=C$^t$Bu$_2$) to $UCl_4$ does not result in the isolation of a hexacoordinate complex. Instead, the aforementioned pentacoordinate complexes are the only species isolated. The inability of **1** or **2** to coordinate a sixth ketimide ligand is likely due to the strongly electron donating nature of the ketimide ligands. This places significant negative charge density on the metal center and disfavors coordination of a sixth ketimide ligand. A similar justification was used to explain the pentacoordinate structures of $[Li(DME)_3][U(NC_5H_{10})_5]$ and $[Li][UR_5]$ (R = $CH_2{}^tBu$, $CH_2SiMe_3$).[32,34]

The solution phase redox properties of complex **2** were investigated by cyclic voltammetry. In THF at room temperature, complex **2** exhibits a reversible redox couple at −2.03 V (vs $Fc/Fc^+$) and a quasi-reversible feature at −0.39 V (vs $Fc/Fc^+$) (see the Supporting Information). We have assigned these features to the U(IV)/(V) couple and the U(V)/(VI) couple, respectively. For comparison, $Cp^*_2U(N{=}CPh_2)_2$ exhibits a U(IV)/(V) redox potential at −0.48 V (vs $Fc/Fc^+$),[39,54] while $Cp^*_2U(N{=}C(Me)Ph)_2$ exhibits a U(IV)/(V) redox potential at −0.54 V (vs $Fc/Fc^+$).[50] Consistent with the cyclic voltammetry results, addition of 0.5 equiv of $I_2$ to **2** generates the neutral five-coordinate U(V) complex, $U(N{=}C^tBu_2)_5$ (**3**) (Scheme 1), which can be isolated by crystallization from concentrated hexanes as a dark brown microcrystalline solid in 63% yield. Complex **3** is exceedingly soluble in hexanes, toluene, and ethereal solvents. Its $^1$H NMR spectrum in $C_6D_6$ consists of a single broad resonance at 1.55 ppm.

Crystals of **3** suitable for X-ray crystallographic analysis were grown from a dilute toluene solution. Complex **3** crystallizes in the monoclinic space group $P2_1/c$, and its solid-state structure is shown in Figure 2. In the solid state, **3** exhibits a trigonal bipyramidal geometry. Its U−N bond lengths range from 2.173(5) to 2.208(4) Å, similar to those observed for complex **2** (avg 2.24 Å) and the uranium(V) amides $[Li(DME)_3][U(NC_5H_{10})_6]$ and $[PPh_4][U(dbabh)_6]$ (Hdbabh = 2,3:5,6-


dx.doi.org/10.1021/ja211875s | J. Am. Chem. Soc. 2012, 134, 4931−4940

**Scheme 1**

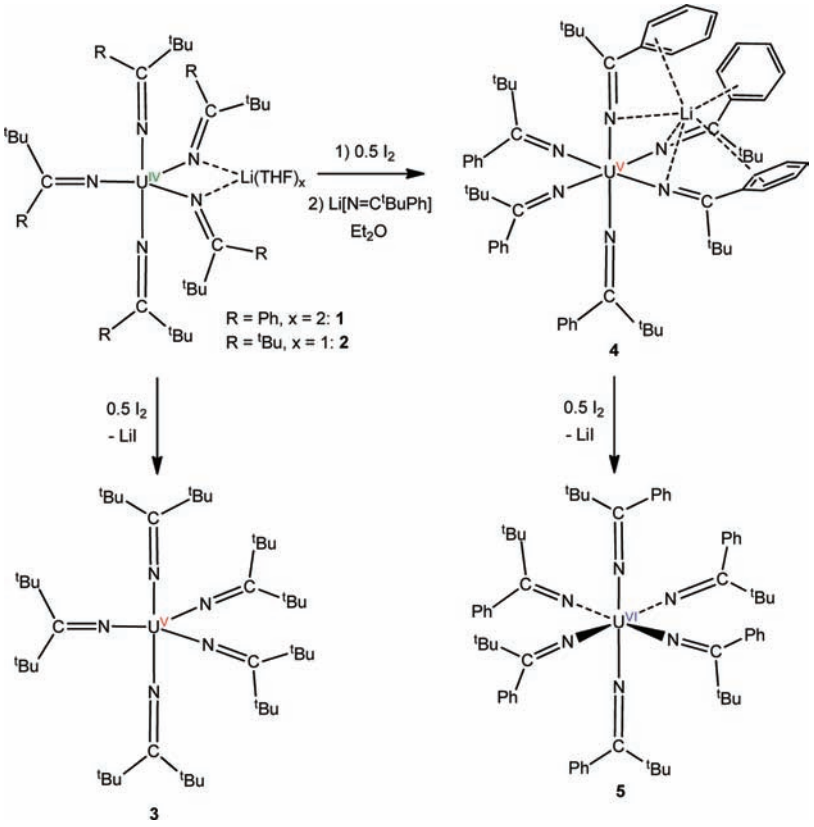


dibenzo-7-azabicyclo[2.2.1]hepta-2,5-diene) (range: 2.23(1) to 2.292(6) Å).[32,60] In addition, **3** exhibits nearly linear U−N−C bond angles ranging from 172.6(4)° to 179.5(5)°, again consistent with sp hybridization at the nitrogen atom. To our knowledge, complex **3** is the first $UX_5$-type complex to be structurally characterized.

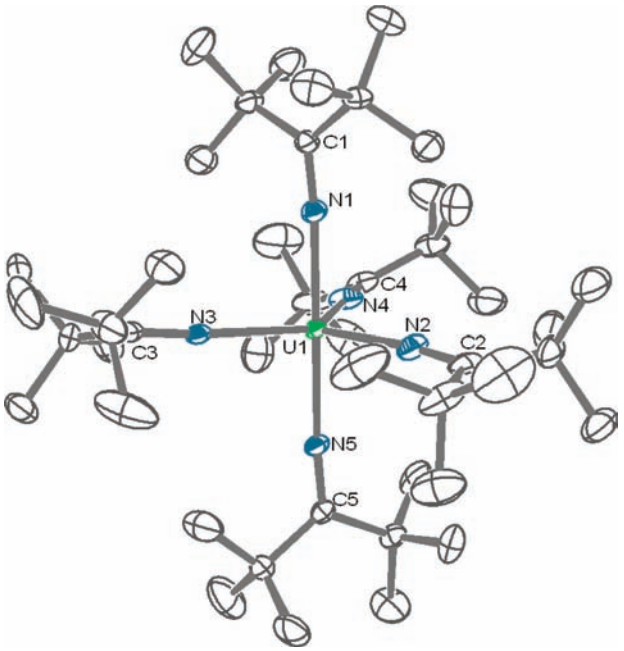


**Figure 2.** Solid-state molecular structure of $U(N{=}C^tBu_2)_5$ (**3**) with 50% probability ellipsoids. Selected bond lengths (Å) and angles (deg): U1−N1 = 2.180(5), U1−N2 = 2.193(5), U1−N3 = 2.208(4), U1−N4 = 2.173(5), U1−N5 = 2.181(5), U1−N1−C1 = 172.6(4), U1−N2−C2 = 172.7(5), U1−N3−C3 = 175.2(4), U1−N4−C4 = 179.5(5), U1−N5−C5 = 175.3(4).

In contrast to the reactivity observed for complex **2**, oxidation of **1** with 0.5 equiv of $I_2$ only results in decomposition. Gratifyingly, however, reaction of **1** with 0.5 equiv of $I_2$ in diethyl ether, followed rapidly by the addition of 1 equiv of $Li(N{=}C^tBuPh)$, results in the formation of the hexacoordinate U(V) complex, $[Li][U(N{=}C^tBuPh)_6]$ (**4**) (Scheme 1), which can be isolated by crystallization from concentrated toluene as dark red blocks in 68% yield. The $^1H$ NMR spectrum of **4** in $C_6D_6$ exhibits resonances at 7.98, 7.66, and 7.57 ppm, attributable to the *meta*, *para*, and *ortho* protons on the phenyl rings, while a resonance at 0.35 ppm is assignable to the *tert*-butyl groups. Additionally, a single resonance at 32.46 ppm is observed in its $^7Li$ NMR spectrum.

Crystals of **4** suitable for X-ray crystallographic analysis were grown from a dilute toluene solution. Complex **4** crystallizes in the rhombohedral space group, $R\bar{3}$, and its solid-state molecular structure is shown in Figure 3. The uranium atom in **4** resides on a site with $S_6$ symmetry, which generates the ketimide ligands in an idealized octahedral geometry. Additionally, the Li cation is disordered over two positions. The U−N bond length is 2.217(2) Å, which is comparable to the bond lengths of the homoleptic uranium(V) amide complexes; $[PPh_4][U(dbabh)_6]$ (2.23(1)−2.27(1) Å) and $[Li(DME)_3][U(NC_5H_{10})_6]$ (2.250(6)−2.292(6) Å)[32,60] but longer than that of the U(V) ketimide complex, $Cp^*_2U(=N\text{-}2,6\text{-}{}^iPr_2C_6H_3)(N{=}CPh_2)$ (2.199(4) Å).[49] The lithium cation is coordinated by three nitrogen atoms of the ketimide ligands and by $\pi$ interactions with the three phenyl rings, which are arranged in a propeller-


dx.doi.org/10.1021/ja211875s | J. Am. Chem. Soc. 2012, 134, 4931−4940

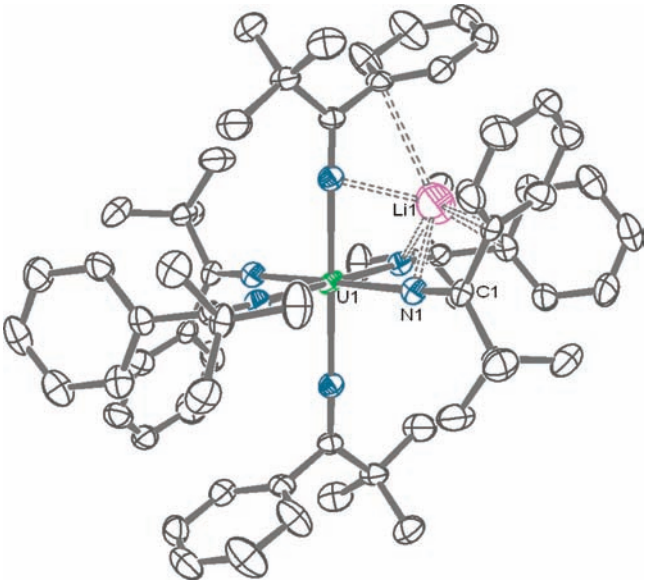


**Figure 3.** ORTEP diagram of $[Li][U(N{=}C^tBuPh)_6]$ (**4**) with 50% probability ellipsoids. Selected bond lengths (Å) and angles (deg): U1−N1 = 2.217(2), U1−N1−C1 = 176.9(2).

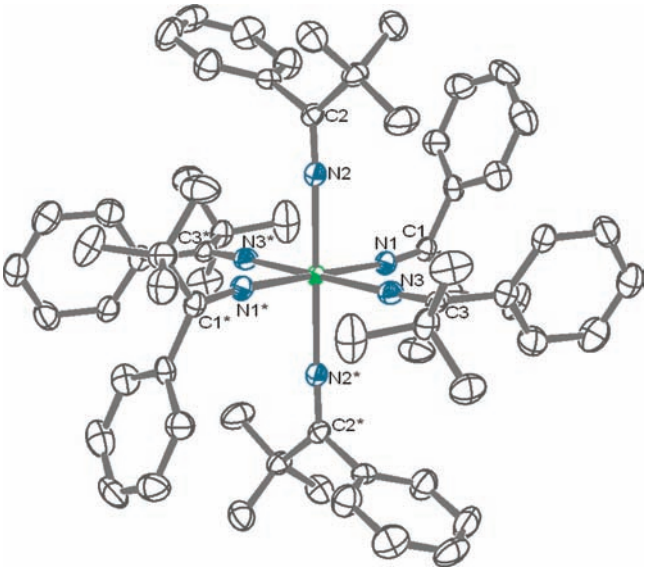


**Figure 4.** ORTEP diagram of $U(N{=}C^tBuPh)_6{\cdot}C_7H_8$ (**5**·$C_7H_8$) with 50% probability ellipsoids. Asterisks denote symmetry related atoms. Toluene solvate omitted for clarity. Selected bond lengths (Å) and angles (deg): U1−N1 = 2.173(3), U1−N2 = 2.175(3), U1−N3 = 2.181(3), U1−N1−C1 = 171.6(3), U1−N2−C2 = 176.3(3), U1−N3−C3 = 178.0(3).

like fashion around the lithium atom. Finally, the U1−N1−C1 bond angle is nearly linear (176.9(2)°), suggestive of sp hybridization at the nitrogen atom.

The cyclic voltammogram of **4**, in THF at room temperature, displays a reversible oxidation feature at −1.52 V (vs $Fc/Fc^+$) which we have assigned to the U(V)/U(VI) redox couple. This value is similar to that of the homoleptic U(V) amide $[Li(DME)_3][U(NC_5H_{10})_6]$ ($E$ = −1.51 V, vs $Fc/Fc^+$)[32] but lower than those reported for analogous alkoxide[33,61] and alkyl complexes,[35] suggesting that the ketimide has a $\pi$-donating ability comparable to that of a di(alkyl)amide ligand. Consistent with the electrochemical data, oxidation of **4** with 0.5 equiv of $I_2$ at −25 °C provides the homoleptic uranium(VI) complex $U(N{=}C^tBuPh)_6$ (**5**) (Scheme 1) in 56% yield. Complex **5** exhibits a $^1H$ NMR spectrum consistent with a diamagnetic complex. For instance, a resonance at 1.46 ppm is assignable to the *tert*-butyl protons, while resonances at 7.11 ppm and 7.35 ppm can be attributed to the aryl protons of the phenyl substitutent. The cyclic voltammogram of **5**, in THF at room temperature, displays a reversible reduction feature at −1.49 V (vs $Fc/Fc^+$) (see the Supporting Information), consistent with the electrochemical parameters observed for complex **4**. Also, present in the cyclic voltammogram of **5** is an irreversible feature at 0.21 V (vs $Fc/Fc^+$), which we have assigned to a ketimide ligand oxidation event.

Crystals of **5** suitable for X-ray crystallographic analysis were grown from a dilute toluene solution. Complex **5** crystallizes in the monoclinic space group $P2_1/n$ as a toluene solvate, **5**·$C_7H_8$. Its solid-state structure is shown in Figure 4. Like complex **4**, **5** adopts an octahedral geometry in the solid-state. Notably, the phenyl substituents are also no longer arranged in a propeller-like fashion, as there is no longer a lithium cation enclosed in the secondary coordination sphere. The U−N bond lengths range from U1−N1 = 2.173(3) Å to U1−N3 = 2.181(3) Å. These bond lengths are comparable to the U−N bond lengths in similar uranium(VI) amides, $U(NC_5H_{10})_6$ and $U(dbabh)_6$ (range: 2.187(6)−2.239(5) Å), but they are shorter than those observed in complex **4**, consistent with the smaller ionic radius of $U^{6+}$.[32,60] As with complexes **1** and **4**, complex **5** exhibits nearly linear U−N−C bond angles, ranging from U1−N1−C1 = 171.6(3)° to U1−N3−C3 = 178.0(3)°, indicative of $\pi$-donation into the metal center.

Attempts to generate a six-coordinate analogue of complex **3** have been unsuccessful, as addition of $Li(N{=}C^tBu_2)$ to **3** results in no reaction. We suggest that the bis(*tert*-butyl) ketimide ligand is likely too bulky to permit formation of an octahedral complex, in contrast to the phenyl-*tert*-butyl ketimide ligand. We have also attempted to oxidize complex **3** by one electron, in an attempt to form the U(VI) cation, $[U(N{=}C^tBu_2)_5]^+$. However, reaction of 3 with a variety of oxidants leads to either decomposition or simply return of starting material.

**Electronic Structure and Bonding.** To better understand the electronic structures of complexes **1** and **4**, their magnetic susceptibilities were measured using SQUID magnetometry. A plot of their effective magnetic moments ($\mu_{eff}$) is shown in Figure 5. Complex **1** exhibits a $\mu_{eff}$ of 2.45 $\mu_B$ at 300 K, much smaller than that of the free $5f^2$ ion, which has a value of 3.58 $\mu_B$.[51,62,63] On cooling to 73 K, the $\mu_{eff}$ value of **1** drops slightly to 2.41 $\mu_B$; however, on further cooling to 4 K, the effective magnetic moment decreases to 0.94 $\mu_B$. This behavior contrasts with that observed for related trigonal bipyramidal U(IV) complexes, $[Li(DME)][U(NC_5H_{10})_5]$ and $[Li][UR_5]$ (R = $CH_2{}^tBu$, $CH_2SiMe_3$),[32,34] but is consistent with the behavior normally observed for U(IV).[34,51,62,64−70] Complex **4** possesses a $\mu_{eff}$ value of 1.38 $\mu_B$ at 300 K, considerably smaller than the 2.54 $\mu_B$ calculated for the $U^{5+}$ ion in a $^2F_{5/2}$ ground state.[49] This value is also lower than those observed for other U(V) complexes, which typically range from 1.9 to 2.5 $\mu_B$ at room temperature.[62,64,71−74] However, it is comparable to the effective magnetic moments found for the homoleptic amido complex $[Li(DME)_3][U(NC_5H_{10})_6]$,[32] and the U(V) alkyl complexes $[Li(DME)_3][U(O^tBu)_2(CH_2SiMe_3)_4]$ and $[Li(DME)_3][U(CH_2SiMe_3)_6]$.[35] On cooling, the $\mu_{eff}$ value of **4** decreases to 1.09 $\mu_B$ at 4 K. This temperature response is in


dx.doi.org/10.1021/ja211875s | J. Am. Chem. Soc. 2012, 134, 4931−4940

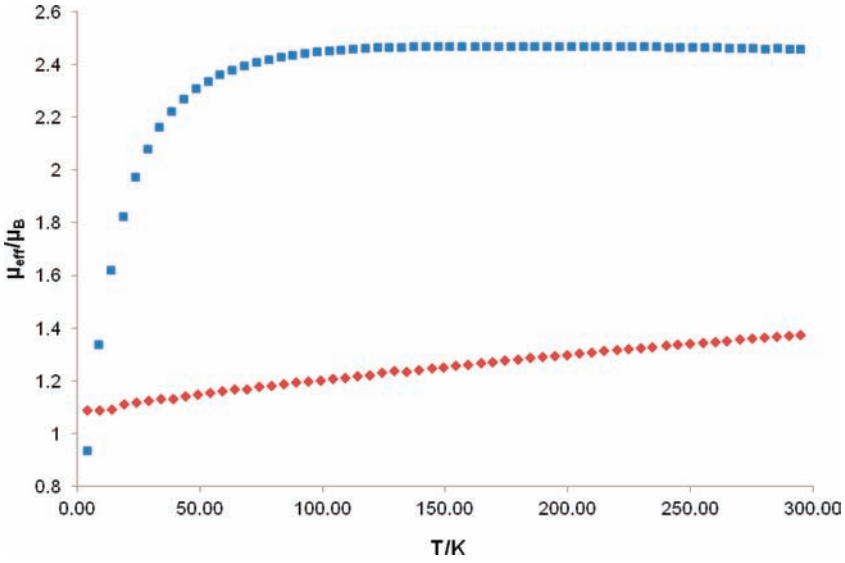


**Figure 5.** Temperature dependent magnetic susceptibility at 1 T for **1** (blue squares) and **4** (red diamonds) from 4 to 300 K.

accord with the magnetic behavior normally observed for U(V).[49,62,64,72,74]

The electronic structure and bonding in **4** were further investigated using a combination of EPR spectroscopy, NIR spectroscopy, and crystal-field modeling. The EPR spectrum of powdered **4** at 2 K is shown in Figure 6 along with the

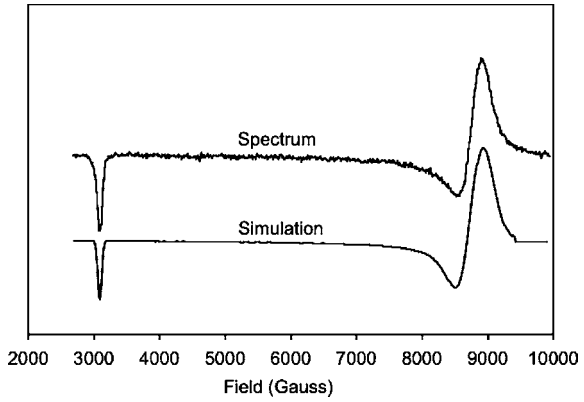


**Figure 6.** EPR spectrum of **4** at 2 K. The complex displays axial symmetry with $g_{\|}$ = 2.132 and $g_{\perp}$ = 0.746.

simulated spectrum. Complex **4** displays axial symmetry with $g_{\|}$ = 2.132 and $g_{\perp}$ = 0.746, which is consistent with the $S_6$ site symmetry of the uranium center in **4**. In addition, $\mu_{eff}$ for the ground state of **4** was determined to be 1.19 $\mu_B$ from the *g*-values using eq 2, slightly greater than the value of 1.09 $\mu_B$ determined by the susceptibility. The good agreement between the values of $\mu_{eff}$ determined by EPR and magnetic susceptibility supports the assignment of the EPR spectrum shown in Figure 6.

$$\mu_{eff} = \frac{\sqrt{g_{\|}^2 + 2g_{\perp}^2}}{2} \qquad (2)$$

The coordination geometry of **4** is very close to octahedral, especially if the substituents on the ketimide ligands are ignored. This geometry enables a more extensive exploration of the bonding in **4** using the approach previously used to describe the bonding in octahedral U(V) halide complexes.[30,31] Although this model is based on pure $O_h$ symmetry, we use it as a starting point for the analysis of the electronic structure of **4** and expect it to provide at least a qualitative picture of the bonding.

In the absence of spin−orbit coupling, the $O_h$ crystal field splits the seven 5f orbitals into a singly degenerate orbital, $a_{2u}$, and two triply degenerate sets of orbitals, $t_{2u}$ and $t_{1u}$. As shown by Burns and Axe, the bonding in octahedral U(V) complexes can be described using three parameters, $\theta$, $\Delta$, and $\zeta$, where $\zeta$ is the spin−orbit coupling constant. In the limit of zero spin−orbit coupling, $\Delta$ is the energy of $t_{2u}$ relative to the $a_{2u}$ orbital, and $t_{1u}$ is destabilized by $\Delta + \theta$ relative to $a_{2u}$.[75] The $a_{2u}$ orbital is nonbonding; the $t_{2u}$ orbital is $\pi$-antibonding with a group overlap corresponding to (5/2) 5f-2p $\pi$-antibonding orbitals; and the $t_{1u}$ orbital is both $\sigma$- and $\pi$-antibonding with a group overlap that corresponds to two 5f-2p $\sigma$-antibonding orbitals and (3/2) 5f-2p $\pi$-antibonding orbitals. Therefore, the strength of a single 5f-2p $\pi$-interaction is $^2/_5\Delta$, and the strength of a single 5f-2p(s) $\sigma$-interaction is $^1/_2\theta + {}^1/_5\Delta$; this information is summarized in Table 1. Spin−orbit coupling splits the $t_{2u}$ state

**Table 1. Bonding and Energetics of the MOs Derived from the 5f-Orbitals in an Octahedral U(V) Complex**

| orbital | group overlap | bonds | energy relative to $a_{2u}$ |
|---|---|---|---|
| $a_{2u}$ | | 0 | |
| $t_{2u}$ | $(5/2)^{1/2}\langle\pi\text{plf}\rangle$ | $^5/_2\pi$ | $\Delta$ |
| $t_{1u}$ | $(3/2)^{1/2}\langle\pi\text{plf}\rangle + (2)^{1/2}\langle\sigma\text{plf}\rangle$ | $^3/_2\pi + 2\sigma$ | $\Delta + \theta$ |

into a $\Gamma_8$ quartet and a $\Gamma_7'$ doublet and splits the $t_{1u}$ state into a $\Gamma_8'$ quartet and a $\Gamma_6$ doublet; the ground $a_{2u}$ state becomes a $\Gamma_7$ doublet when spin−orbit coupling is included. A useful schematic of this orbital picture can be found in ref 31. For an octahedral complex, $\theta$, $\Delta$, and $\zeta$ may be determined if the NIR spectrum can be assigned to determine the energies of the low-lying $\Gamma_7'$, $\Gamma_8'$, and $\Gamma_6$ excited states (the energy of $\Gamma_8$ is too low to be observed in the present study). In **4**, the symmetry is lowered from octahedral due to the fact that the ketimide ligand is not axially symmetric and therefore not a $\pi$-donor along both the *x*- and *y*-axes (taking the U−N vector as the *z*-


dx.doi.org/10.1021/ja211875s | J. Am. Chem. Soc. 2012, 134, 4931−4940

axis). Each of the $\Gamma_8$ and $\Gamma_8'$ quartets are split into two doublets by this asymmetry with respect to $\pi$-bonding. Keeping this in mind, the NIR spectrum of **4** may be assigned as shown in Figure 7. Note that the parameters $\Delta$ and $\theta$ are linearly related

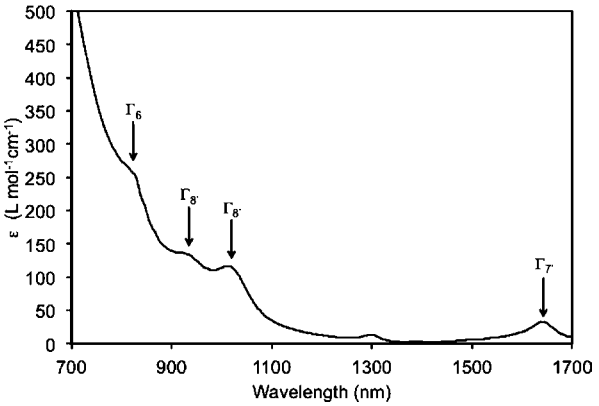


**Figure 7.** NIR spectrum of **4** showing assignments of the transitions to low-lying excited states with their labels for octahedral symmetry. The $\Gamma_8'$ state is split by the lower symmetry of **4**. The peak at 1300 $cm^{-1}$ is due to a ligand-based absorption (see Figure S21 of the Supporting Information).

to the more general crystal field parameters $B^4_0$ and $B^6_0$ (defined using the Wybourne convention).[76]

If the energies of the transitions assigned to the split $\Gamma_8'$ state are averaged, the values for $\theta$ and $\Delta$ are determined to be 5100 ± 990 $cm^{-1}$ and 1920 ± 1456 $cm^{-1}$, respectively, with $\zeta$ set equal to 1800 $cm^{-1}$. The value of $\zeta$ was chosen such that both the NIR and EPR data were well modeled by the crystal field parameters. It should be noted that the values of $\theta$ and $\Delta$ depend on the value of $\zeta$. The assignment of the NIR spectrum was checked by transforming the octahedral coordinate system to a $C_{3v}$ system (the $z$-axis is the U−Li vector). The distortion from $O_h$ symmetry was modeled by changing the $B^2_0$ parameter, which is zero in $O_h$ symmetry, and fitting the optical spectrum by allowing the $B^4_3$ and $B^6_3$ parameters to vary, which splits the $\Gamma_8'$ state. The best agreement with the EPR data was found for $B^2_0$ set equal to 2400 $cm^{-1}$; the experimental and calculated observables are given in Table 2,

**Table 2. Experimental and Calculated Observables for 4 Determined with $B^2_0$ = 2400 $cm^{-1}$, $B^4_3$ = 11230 $cm^{-1}$, and $B^6_3$ = 4460 $cm^{-1}$**

| observable | exptl | calcd |
|---|---|---|
| $g_\parallel$ | 2.132 | 2.123 |
| $g_\perp$ | 0.746 | 0.796 |
| $\Gamma_7'$ | 6080 $cm^{-1}$ | 6290 $cm^{-1}$ |
| $\Gamma_8'$ | 9843 $cm^{-1}$ | 9740 $cm^{-1}$ |
| $\Gamma_8'$ | 10850 $cm^{-1}$ | 10560 $cm^{-1}$ |
| $\Gamma_6$ | 12195 $cm^{-1}$ | 12520 $cm^{-1}$ |

and the combined crystal field parameters are given in Table S5 of the Supporting Information. The experimental and calculated values agree to within 350 $cm^{-1}$ (1 kcal·$mol^{-1}$), which permits a reasonable estimate of the strengths of the $\sigma$ and $\pi$ interactions between the uranium 5f-orbitals and the ketimide ligands. The magnetic moment as a function of temperature may be calculated from the crystal field parameters (Figure S34) and is in reasonable agreement with experiment. The main difference between calculation and experiment is that the EPR spectrum that is used as the basis for the calculation corresponds to a moment ∼10% greater than the measured moment, which leads to the calculated moment being ∼10% larger than the measured moment.

Using the relationships in Table 2 and the crystal field data in Table 3, the strength of the interactions between the uranium 5f orbitals and the nitrogen 2p orbitals may be estimated. It should be noted that one of the parameters, $\zeta$, was not permitted to freely vary, which could result in a systematic error. In addition, the large standard deviations in the values of the crystal field parameters (given in parentheses in Table 3) result in relatively large errors in the bond strengths, so the results are largely qualitative. Using the data in Table 2, the ketimide $\sigma$-bond strength is 8 ± 2 kcal·$mol^{-1}$, and the strength of the $\pi$-interaction is 2 ± 1 kcal·$mol^{-1}$. However, complex **4** has only half of the 2p-5f $\pi$-interactions as the $UX_6^-$ complexes upon which the model is based, so the strength of the 2p-5f $\pi$-interaction in **4** is actually 4 ± 3 kcal $mol^{-1}$, double that given by the relationships in Table 2. The corrected values of the $\sigma$- and $\pi$-interactions are given in Table 3, along with the values for $UX_6^-$ determined using the relationships in Table 2. Regardless of the large errors in the strengths of the 5f-2p interactions for the ketimide ligand, it is clear that they are relatively weak and, surprisingly, are comparable to those observed for $[UX_6]^-$ (X = F, Cl, Br). While these values seem to imply that the interactions between U(V) and the ketimide ligands are weak, it should be remembered that the uranium 6d orbitals may interact more strongly with the ligands than do the 5f orbitals,[8,9,77−79] and the values given here reflect only the contribution of the 5f orbitals to metal−ligand bonding.[80]

## ■ CONCLUDING REMARKS

In this contribution we report the synthesis and characterization of a series of homoleptic ketimide complexes, including the high valent species $U(N{=}C^tBu_2)_5$, $[Li][U(N{=}C^tBuPh)_6]$, and $U(N{=}C^tBuPh)_6$. Their isolation further demonstrates that the ketimide ligand platform is strongly electron donating and capable of stabilizing high oxidation states. A cyclic voltammetry study of $[Li][U(N{=}C^tBuPh)_6]$ suggests that the ketimide ligand is similar to a di(alkyl)amide ligand in terms of electron donating ability. As with the amide ligand, the ketimide ligand is likely both a strong $\sigma$ and $\pi$ donor. However, analysis of the electronic structure of $[Li][U(N{=}C^tBuPh)_6]$ reveals that the strength of the $\sigma$- and $\pi$-interactions between the ligand 2p and the uranium 5f orbitals is similar to those exhibited by $[UX_6]^-$ (X = F, Cl, Br). This similarity suggests that uranium 5f participation in the bonding of $[UX_6]^-$-type complexes does not vary widely among the complexes examined here and that the seemingly strong uranium−ketimide interaction (as evidenced by the low U(V)/U(VI) redox potential, for example) may be due to the participation of the uranium 6d orbitals. For future work we will attempt to quantify the level of 6d participation in the bonding of this class of materials.

## ■ EXPERIMENTAL SECTION

**General.** All reactions and subsequent manipulations were performed under anaerobic and anhydrous conditions either under a high vacuum or an atmosphere of argon or nitrogen. Diethyl ether, hexanes, toluene, and THF were dried using a Vacuum Atmospheres DRI-SOLV Solvent Purification system. DME was distilled from sodium benzophenone ketyl. All deuterated solvents were purchased


dx.doi.org/10.1021/ja211875s | J. Am. Chem. Soc. 2012, 134, 4931−4940

**Table 3. Crystal Field Splitting Data for a Series of U(V) Complexes**

| complex | $\theta$ ($cm^{-1}$) | $\Delta$ ($cm^{-1}$) | $\zeta$ ($cm^{-1}$) | 2p-5f $\sigma$ (kcal $mol^{-1}$) | 2p-5f $\pi$ (kcal $mol^{-1}$) |
|---|---|---|---|---|---|
| $[UF_6]^-$ | 6882[a] | 4479 | 1885 | 12 | 5 |
| $[UCl_6]^-$ | 3371 | 2963 | 1931 | 7 | 3 |
| $[UBr_6]^-$ | 2375 | 2935 | 1925 | 5 | 3 |
| $[U(N{=}C^tBuPh)_6]^-$ | 5100(990)[b] | 1920(1456)[b,c] | 1800 | 8(2) | 4(3)[d] |

[a]Data for $[UX_6]^-$ (X = F, Cl, Br) from ref 31. [b]The value in parentheses is the standard deviation from the crystal field model. [c]The value appears low because **4** has half the $\pi$-interactions of $UX_6^-$. [d]The value is doubled due to the fact that **4** has half the $\pi$-interactions of $UX_6^-$.

from Cambridge Isotope Laboratories Inc. and were dried over activated 4 Å molecular sieves for 24 h prior to use. $UCl_4$,[81] Li(N=C$^t$Bu$_2$), and Li(N=C$^t$BuPh) were synthesized according to published procedures.[44,82,83] All other reagents were obtained from commercial sources and used as received.

NMR spectra were recorded on a Varian UNITY INOVA 500 spectrometer or a Bruker Avance III Ultashield Plus 800 spectrometer. $^1$H and $^{13}$C{$^1$H} NMR spectra are referenced to external $SiMe_4$ using the residual protio solvent peaks as internal standards ($^1$H NMR experiments) or the characteristic resonances of the solvent nuclei ($^{13}$C NMR experiments). $^7$Li{$^1$H} NMR spectra are referenced to an external saturated solution of LiCl in deuterium oxide. Elemental analyses were performed at the Micro-Mass Facility at the University of California, Berkeley. UV−vis/NIR spectra were recorded on a UV-3600 Shimadzu spectrophotometer. IR spectra were recorded on a Mattson Genesis FTIR or a Thermo Scientific Nicolet 6700 FT-IR spectrometer.

**Cyclic Voltammetry Measurements.** CV experiments were performed using a CH Instruments 600c Potentiostat, and the data were processed using CHI software (version 6.29). All experiments were performed in a glovebox using a 20 mL glass vial as the cell. The working electrode consisted of a platinum disk embedded in glass (2 mm diameter), and both the working and reference electrodes consisted of a platinum wire. Solutions employed during CV studies were typically 1 mM in the uranium complex and 0.1 M in $[Bu_4N][PF_6]$. All potentials are reported versus the $[Cp_2Fe]^{0/+}$ couple.

**Magnetism Measurements.** Magnetism data were recorded using a Quantum Design MPMS 5XL SQUID magnetometer. All experiments were performed between 4 and 300 K using 50−100 mg of powdered, crystalline solid. Samples were loaded into NMR tubes, which were subsequently flame-sealed. The solid was kept in place with approximately 80 mg of quartz wool packed on either side of the sample. The data was corrected for the contribution of the NMR tube holder and the quartz wool. The experiment for **1** was performed using a 1 T field. Diamagnetic corrections ($\chi_{dia} = -7.29 \times 10^{-4}$ $cm^3 \cdot mol^{-1}$ for **1**, $\chi_{dia} = -7.33 \times 10^{-4}$ $cm^3 \cdot mol^{-1}$ for **4**) were made using Pascal's constants.[84] The magnetization of **4** was corrected for the presence of a ferromagnetic impurity using data taken at 0.5, 1, and 3 T in combination with eq 3, where $M_{sample}(T)$ and $M_{measured}(T)$ are the magnetization of the sample and measured magnetization, respectively, and $M_{ferro}$ is the magnetization of the ferromagnetic impurity, which is field and temperature independent.

$$M_{sample}(T) = M_{measured}(T) - M_{ferro} \quad (3)$$

**EPR Spectroscopy.** EPR spectra were obtained at 2 K with a Varian E-12 spectrometer equipped with a flowing liquid He cryostat, an EIP-547 microwave frequency counter, and a Varian E-500 gaussmeter, which was calibrated using 2,2-diphenyl-1-picrylhydrazyl (DPPH, $g = 2.0036$). The spectrum was fit using a version of the code ABVG modified to use a pseudo-Voigt line shape and modified to fit spectra using the downhill simplex method.

**Crystal Field Calculations.** The Hamiltonian and matrix elements for an $f^1$ configuration in $O_h$ symmetry have been given many times (see, for example, ref 85). The conversion of the $O_h$ crystal field parameters to $C_{3v}$ symmetry is described by Görller-Walrand and Binnemans.[86] The calculated magnetic susceptibility was determined from the Van Vleck susceptibility equation using the energies and eigenvectors obtained with the parameters given in Table 2 for the best fit to the optical spectrum and the EPR $g$ values.[87]

**[Li(THF)$_2$][U(N=C$^t$BuPh)$_5$] (1).** To a stirring solution of $UCl_4$ (0.2709 g, 0.71 mmol) in THF (3 mL) was added dropwise a solution of Li(N=C$^t$BuPh) (0.602 g, 3.61 mmol) in THF (3 mL). The reaction mixture immediately turned dark brown. After stirring for 15 min, the solvent was removed in vacuo to afford a dark brown powder. The solid was dissolved in hexanes, and a white precipitate was removed by filtration of the solution through a Celite column (2 cm × 0.5 cm) supported on glass wool. The filtrate was concentrated in vacuo and stored at −25 °C for 24 h to afford dark brown crystals. 0.6009 g, 71% yield. $^1$H NMR (500 MHz, 25 °C, $C_6D_6$): $\delta$ −5.01 (s, 45H, $^t$Bu), 0.28 (s, 8H, $\beta$-THF), 1.35 (s, 8H, $\alpha$-THF), 7.43 (s, 10H, $m$-CH), 7.73 (s, 5H, $p$-CH), 12.33 (s, 10H, $o$-CH). $^7$Li{$^1$H} NMR (194 MHz, 25 °C, $C_6D_6$): $\delta$ 14.52 (s). Anal. Calcd for $C_{63}H_{86}LiN_5O_2U$: C, 63.57, H, 7.28, N, 5.88. Found: C, 63.19, H, 7.06, N, 5.91. IR (KBr pellet, $cm^{-1}$): 1632(s, br), 1583(sh), 1487(sh), 1477(m), 1471(m), 1443(m), 1392(m), 1358(m), 1311(w), 1254(sh), 1217(m), 1192(s), 1161(sh), 1072(m), 1057(m), 1054(m), 1018(w), 991(w), 945(s), 903(s), 872(sh), 858(w), 822(w), 775(s), 733(sh), 704(s), 688(sh), 623(m), 609(sh), 561(m), 515(w), 484(sh), 444(m). UV−vis/NIR (DME, 4.9 mM, 25 °C): 736 (sh, $\varepsilon$ = 311.0 $L \cdot mol^{-1} \cdot cm^{-1}$), 850 (sh, $\varepsilon$ = 121.1 $L \cdot mol^{-1} \cdot cm^{-1}$), 986 ($\varepsilon$ = 121.6 $L \cdot mol^{-1} \cdot cm^{-1}$), 1156 ($\varepsilon$ = 221.5 $L \cdot mol^{-1} \cdot cm^{-1}$), 1284 ($\varepsilon$ = 153.2 $L \cdot mol^{-1} \cdot cm^{-1}$), 1416 ($\varepsilon$ = 109.5 $L \cdot mol^{-1} \cdot cm^{-1}$), 1562 ($\varepsilon$ = 75.5 $L \cdot mol^{-1} \cdot cm^{-1}$).

**[Li(THF)][U(N=C$^t$Bu$_2$)$_5$] (2).** To a stirring solution of $UCl_4$ (0.221 g, 0.58 mmol) in THF (3 mL) was added dropwise a suspension of Li(N=C$^t$Bu$_2$) (0.433 g, 2.94 mmol) in THF (3 mL). The reaction mixture immediately turned dark brown. The reaction mixture was allowed to stir at room temperature for 1 h, after which the solvent was removed in vacuo, affording a dark brown solid. The solid was dissolved in hexanes, and the solution was filtered through a Celite column (2 cm × 0.5 cm) supported on glass wool. The filtrate was concentrated in vacuo and stored at −25 °C for 24 h, resulting in the deposition of dark-brown crystals. 0.3965 g, 67% yield. $^1$H NMR (500 MHz, 25 °C, $C_6D_6$): $\delta$ −1.47 (s, 90H, $^t$Bu), 1.56 (s, 4H, $\beta$-THF), 4.24 (s, 4H, $\alpha$-THF). $^7$Li{$^1$H} NMR (194 MHz, 25 °C, $C_6D_6$): $\delta$ 89.38 (s). Anal. Calcd for $C_{49}H_{98}LiN_5OU$: C, 57.80; H, 9.70; N, 6.88. Found: C, 57.11; H, 9.61; N, 7.28. IR (KBr pellet, $cm^{-1}$): 1616(s, br), 1505(sh), 1481(s), 1465(sh), 1448(sh), 1384(s), 1360(s), 1335(w), 1304(w), 1214(s), 1037(s), 955(s), 928(sh), 882(w), 839(w), 808(w), 806(w), 724(w), 682(s), 674(sh), 555(s), 491(w), 484(w), 435(m), 428(sh). UV−vis/NIR (DME, 4.9 mM, 25 °C): 890 (sh, $\varepsilon$ = 116.7 $L \cdot mol^{-1} \cdot cm^{-1}$), 1012 ($\varepsilon$ = 93.1 $L \cdot mol^{-1} \cdot cm^{-1}$), 1158 ($\varepsilon$ = 111.1 $L \cdot mol^{-1} \cdot cm^{-1}$), 1248 ($\varepsilon$ = 107.3 $L \cdot mol^{-1} \cdot cm^{-1}$), 1378 ($\varepsilon$ = 63.6 $L \cdot mol^{-1} \cdot cm^{-1}$), 1592 (sh, $\varepsilon$ = 104.3 $L \cdot mol^{-1} \cdot cm^{-1}$).

**U(N=C$^t$Bu$_2$)$_5$ (3).** To a cold (−25 °C), stirring solution of **2** (0.297 g, 0.29 mmol) in $Et_2O$ (4 mL) was added dropwise a solution of $I_2$ (0.037 g, 0.15 mmol) in $Et_2O$ (2 mL). The reaction mixture was stirred for 5 min, after which the solvent was removed in vacuo to afford a dark brown solid. Dissolution of the solid in hexanes was followed by removal of a white precipitate by filtration of the solution through a Celite column (2 cm × 0.5 cm) supported on glass wool. The solution was stored at −25 °C for 24 h, resulting in the formation of dark red brown crystals. 0.1726 g, 63% yield. X-ray quality crystals were grown from a dilute solution of **3** in toluene. $^1$H NMR (500 MHz, 25 °C, $C_6D_6$): $\delta$ 1.55 (br s, 90H, $^t$Bu). Anal. Calcd for $C_{45}H_{90}N_5U$: C, 57.54; H, 9.66; N, 7.46. Found: C, 57.12; H, 9.47; N,


dx.doi.org/10.1021/ja211875s | J. Am. Chem. Soc. 2012, 134, 4931−4940

**Table 4. X-ray Crystallographic Data for Complexes 1−4 and 5·$C_7H_8$**

| | 1 | 2 | 3 | 4 | 5·$C_7H_8$ |
|---|---|---|---|---|---|
| empirical formula | $C_{63}H_{86}LiN_5O_2U$ | $C_{49}H_{98}LiN_5OU$ | $C_{45}H_{90}N_5U$ | $C_{66}H_{84}LiN_6U$ | $C_{73}H_{92}N_6U$ |
| crystal habit, color | block, brown | block, brown | plate, brown | brick, dark red | brick, dark green |
| crystal size (mm) | 0.30 × 0.20 × 0.15 | 0.1 × 0.05 × 0.05 | 0.20 × 0.10 × 0.02 | 0.40 × 0.25 × 0.25 | 0.45 × 0.35 × 0.2 |
| crystal system | triclinic | monoclinic | monoclinic | hexagonal | monoclinic |
| space group | $P\bar{1}$ | $P2_1/c$ | $P2_1/c$ | $R\bar{3}$ | $P2_1/n$ |
| volume (Å$^3$) | 2961.8(5) | 5242.0(3) | 9702(2) | 4635.7(4) | 3248.6(6) |
| $a$ (Å) | 13.2886(13) | 13.8905(4) | 20.967 (3) | 12.1214(8) | 14.2791(16) |
| $b$ (Å) | 13.9258(14) | 14.6036(4) | 19.715(3) | 12.1214(8) | 11.9428(14) |
| $c$ (Å) | 18.2372(17) | 25.8603(7) | 23.470(3) | 36.432(3) | 19.064(2) |
| $\alpha$ (deg) | 76.405(5) | 90 | 90 | 90 | 90 |
| $\beta$ (deg) | 77.740(5) | 92.1840(10) | 90.215 (8) | 90 | 92.216(2) |
| $\gamma$ (deg) | 65.596(4) | 90 | 90 | 120 | 90 |
| $Z$ | 2 | 4 | 8 | 3 | 2 |
| formula weight (g/mol) | 1190.34 | 1018.29 | 939.25 | 1206.36 | 1291.56 |
| density (calcd) (mg/m$^3$) | 1.335 | 1.290 | 1.286 | 1.296 | 1.320 |
| absorption coeff (mm$^{-1}$) | 2.785 | 3.133 | 3.378 | 2.668 | 2.544 |
| $F_{000}$ | 1220 | 2120 | 3896 | 1851 | 1328 |
| total no. reflections | 28902 | 47640 | 65831 | 9511 | 27029 |
| unique reflections | 14614 | 15852 | 19821 | 1779 | 6565 |
| final $R$ indices [$I > 2\sigma(I)$] | $R_1$ = 0.0452, $wR_2$ = 0.1081 | $R_1$ = 0.0293, $wR_2$ = 0.0771 | $R_1$ = 0.0410, $wR_2$ = 0.0922 | $R_1$ = 0.0270, $wR_2$ = 0.0524 | $R_1$ = 0.0272, $wR_2$ = 0.0626 |
| largest diff. peak and hole (e$^-$ Å$^{-3}$) | 5.918 and −3.774 | 1.473 and −1.369 | 1.862 and −1.149 | 0.670 and −0.486 | 0.872 and −0.753 |
| GOF | 1.116 | 0.979 | 1.058 | 1.071 | 0.980 |

7.27. IR (KBr pellet, cm$^{-1}$): 1763(w), 1689(w), 1610(s, br), 1481(s), 1470(m), 1446(sh), 1385(m), 1358(s), 1335(w), 1267(w), 1213(s), 1038(m), 957(s), 939(m), 904(sh), 891(w), 841(w), 796(w), 791(w), 739(w), 685(s), 550(s), 434(s). UV−vis/NIR (DME, 4.3 mM, 25 °C): 904 (sh, $\varepsilon$ = 231.8 L·mol$^{-1}$·cm$^{-1}$), 1022 ($\varepsilon$ = 146.3 L·mol$^{-1}$·cm$^{-1}$), 1272 ($\varepsilon$ = 135.1 L·mol$^{-1}$·cm$^{-1}$), 1604 ($\varepsilon$ = 204.0 L·mol$^{-1}$·cm$^{-1}$).

**[Li][U(N═C$^t$BuPh)$_6$] (4).** To a cold (−25 °C), stirring solution of **1** (0.1345 g, 0.11 mmol) in $Et_2O$ (8 mL) was added dropwise a solution of $I_2$ (0.015 g, 0.06 mmol) in $Et_2O$ (2 mL). The reaction mixture was stirred for 5 min, whereupon a suspension of Li(N═C$^t$BuPh) (0.019 mg, 0.11 mmol) in $Et_2O$ (8 mL) was added dropwise. The reaction mixture was then stirred for an additional 5 min, after which the solvent was removed in vacuo, affording a dark red solid. Dissolution of the solid in toluene (5 mL) was followed by removal of a gray precipitate by filtration through a Celite column (2 cm × 0.5 cm) supported on glass wool. The solution was concentrated in vacuo and stored at −25 °C for 24 h, resulting in the formation of dark red crystals. 0.0921 g, 68% yield. Crystals of **4** suitable for X-ray analysis were grown from a dilute hexanes solution. $^1$H NMR (500 MHz, 25 °C, $C_6D_6$): $\delta$ 0.35 (s, 54H, $^t$Bu), 7.57 (s, 12H, *m*-CH), 7.66 (s, 6H, *p*-CH), 7.98 (s, 12H, *o*-CH). $^7$Li{$^1$H} NMR (194 MHz, 25 °C, $C_6D_6$): $\delta$ 32.46 (s). Anal. Calcd $C_{66}H_{84}LiN_6U$: C, 65.71, H, 7.02, N, 6.97. Found: C, 65.34, H, 6.96, N 6.85. IR (KBr pellet, cm$^{-1}$): 1664(sh), 1642(sh), 1627(s), 1600(sh), 1581(sh), 1475(m), 1464(m), 1455(m), 1391(m), 1361(m), 1263(w), 1217(w), 1195(s), 1111(w, br), 1073(w), 1030(m), 944(s), 907(s), 772(s), 706(s), 623(w), 564(m), 442(m). UV−vis/NIR (DME, 3.8 mM, 25 °C): 814 (sh, $\varepsilon$ = 264 L·mol$^{-1}$·cm$^{-1}$), 930 (sh, $\varepsilon$ = 135 L·mol$^{-1}$·cm$^{-1}$), 1018 ($\varepsilon$ = 116 L·mol$^{-1}$·cm$^{-1}$), 1300 ($\varepsilon$ = 13 L·mol$^{-1}$·cm$^{-1}$), 1644 ($\varepsilon$ = 32 L·mol$^{-1}$·cm$^{-1}$).

**U(N═C$^t$BuPh)$_6$ (5).** To a cold (−25 °C), stirring solution of **4** (0.098 g, 0.08 mmol) in $Et_2O$ (3 mL) was added dropwise a solution of $I_2$ (0.011 g, 0.04 mmol) in $Et_2O$ (1 mL). The solution was stirred for 5 min, and the solvent was removed in vacuo, affording a dark green solid. The solid was dissolved in toluene (3 mL), and a white precipitate was removed by filtration of the solution through a Celite column (2 cm × 0.5 cm) supported on glass wool. The solution was concentrated in vacuo and cooled to −25 °C for 24 h, resulting in the deposition of dark green crystals. 0.0585 g, 56% yield. X-ray quality crystals of **5** were grown from a dilute solution in toluene. $^1$H NMR (500 MHz, 25 °C, $C_6D_6$): $\delta$ 1.46 (s, 54H, $CH_3$), 7.11 (m, 6H, *p*-CH), 7.35 (m, 24H, *o*-CH and *m*-CH). $^{13}$C{$^1$H} NMR (201 MHz, 25 °C, $C_6D_6$): $\delta$ 180.40 (s, C═N), 164.93 (s, *ipso*-C), 128.38 (s, *o*-CH), 126.55 (s, *m*-CH), 125.76 (s, *p*-CH), 72.81 (s, $C(CH_3)_3$), 27.90 (s, $C(CH_3)_3$). Anal. Calcd for $C_{66}H_{84}N_6U$: C, 66.09, H, 7.06, N, 7.01. Found: C, 65.34, H, 7.06, N 6.87. IR (KBr pellet, cm$^{-1}$): 1622(s, br), 1579(sh), 1564(sh), 1556(m), 1532(sh), 1496(sh), 1487(m), 1474(s), 1468(s), 1440(s), 1389(m), 1359(m), 1257(m), 1215(s), 1197(s), 1182(sh), 1164(w), 1072(m), 1027(m), 1001(w), 942(s), 904(s), 847(w), 837(w), 774(s), 737(m), 704(s), 671(sh), 619(s), 560(s), 467(w), 444(s).

**X-ray Crystallography.** Data for **4** and **5**·$C_7H_8$ were collected on a Bruker 3-axis platform diffractometer equipped with a SMART-1000 CCD detector using a graphite monochromator with a Mo K$\alpha$ X-ray source ($\alpha$ = 0.71073 Å). A hemisphere of data was collected using $\omega$ scans with 0.3° frame widths. Frame exposures of 20 s were used for both complexes **4** and **5**·$C_7H_8$. Data for **1**, **2**, and **3** were collected on a Bruker KAPPA APEX II diffractometer equipped with an APEX II CCD detector using a TRIUMPH monochromator with a Mo K$\alpha$ X-ray source ($\alpha$ = 0.71073 Å). The crystals of **1**, **2**, and **3** were mounted on a cryoloop under Paratone-N oil, and all data were collected at 100(2) K using an Oxford nitrogen gas cryostream system. Frame exposures of 10 and 20 s were used for **2** and **3**, respectively, while frame exposures of 10 and 15 s were used for **1**. Data collection and cell parameter determination were conducted using the SMART program.[88] Integration of the data frames and final cell parameter refinement were performed using SAINT software.[89] Absorption correction of the data for **1**, **2**, and **3** was carried out using the multiscan method SADABS,[90] while the absorption correction of the data for **4** and **5** was carried out empirically on the basis of reflection $\psi$-scans. Subsequent calculations were carried out using SHELXTL.[91] Structure determination was done using direct or Patterson methods and difference Fourier techniques. All hydrogen atom positions were idealized, and rode on the atom of attachment with exceptions noted in the subsequent paragraph. Structure solution, refinement, graphics, and creation of publication materials were performed using SHELXTL.[91] A summary of relevant crystallographic data is presented in Table 4.

For complex **1**, a *tert*-butyl group was found to be disordered between two positions about the tertiary carbon, in a 50:50 ratio. In complex **2**, two *tert*-butyl groups were disordered about their tertiary carbons, each in a 44:56 ratio. Hydrogen atom positions were not assigned to disordered carbon atoms. For complex **4**, the single Li cation was disordered over two sites in a 50:50 ratio, while for complex **5**, a toluene molecule was disordered over two sites in a 50:50 ratio.

## ■ ASSOCIATED CONTENT

### Supporting Information

Experimental procedures, crystallographic details (as CIF files), magnetic susceptibility plots, tabulated cyclic voltammetry data, and spectral data for **1**−**5**. This material is available free of charge via the Internet at http://pubs.acs.org.

## ■ AUTHOR INFORMATION


### Corresponding Author

hayton@chem.ucsb.edu; wwlukens@lbl.gov; nmedelstein@lbl.gov


### Notes

The authors declare no competing financial interest.

## ■ ACKNOWLEDGMENTS

Research at UCSB was supported by the U.S. Department of Energy, Office of Basic Energy Sciences, Chemical Sciences, Biosciences, and Geosciences Division under Contract No. DE-FG02-09ER16067, and by the National Science Foundation under Award No. 1059097. Portions of this work were supported by U.S. Department of Energy, Basic Energy Sciences, Chemical Sciences, Biosciences, and Geosciences Division and were performed at Lawrence Berkeley National Laboratory under Contract No. DE-AC02-05CH11231. We also thank Skye Fortier and Richard Lewis for assistance with the SQUID magnetization measurements.

## ■ REFERENCES


(1) Denning, R. G.; Green, J. C.; Hutchings, T. E.; Dallera, C.; Tagliaferri, A.; Giarda, K.; Brookes, N. B.; Braicovich, L. *J. Chem. Phys.* **2002**, *117*, 8008−8021.

(2) Denning, R. G. *J. Phys. Chem. A* **2007**, *111*, 4125−4143.

(3) Prodan, I. D.; Scuseria, G. E.; Martin, R. L. *Phys. Rev. B* **2007**, *76*, 033101.

(4) Kozimor, S. A.; Yang, P.; Batista, E. R.; Boland, K. S.; Burns, C. J.; Clark, D. L.; Conradson, S. D.; Martin, R. L.; Wilkerson, M. P.; Wolfsberg, L. E. *J. Am. Chem. Soc.* **2009**, *131*, 12125−12136.

(5) Cantat, T.; Graves, C. R.; Jantunen, K. C.; Burns, C. J.; Scott, B. L.; Schelter, E. J.; Morris, D. E.; Hay, P. J.; Kiplinger, J. L. *J. Am. Chem. Soc.* **2008**, *130*, 17537−17551.

(6) Li, J.; Bursten, B. E. *J. Am. Chem. Soc.* **1997**, *119*, 9021−9032.

(7) Tassell, M. J.; Kaltsoyannis, N. *Dalton Trans.* **2010**, *39*, 6719−6725.

(8) Ingram, K. I. M.; Kaltsoyannis, N.; Gaunt, A. J.; Neu, M. P. *J. Alloys Compd.* **2007**, *444*−*445*, 369−375.

(9) Ingram, K. I. M.; Tassell, M. J.; Gaunt, A. J.; Kaltsoyannis, N. *Inorg. Chem.* **2008**, *47*, 7824−7833.

(10) Gaunt, A. J.; Reilly, S. D.; Enriquez, A. E.; Scott, B. L.; Ibers, J. A.; Sekar, P.; Ingram, K. I. M.; Kaltsoyannis, N.; Neu, M. P. *Inorg. Chem.* **2007**, *47*, 29−41.

(11) Jensen, M. P.; Bond, A. H. *J. Am. Chem. Soc.* **2002**, *124*, 9870−9877.

(12) Arliguie, T.; Belkhiri, L.; Bouaoud, S.-E.; Thuery, P.; Villiers, C.; Boucekkine, A.; Ephritikhine, M. *Inorg. Chem.* **2009**, *48*, 221−230.

(13) Roger, M.; Belkhiri, L.; Arliguie, T.; Thuery, P.; Boucekkine, A.; Ephritikhine, M. *Organometallics* **2008**, *27*, 33−42.

(14) Schnaars, D. D.; Batista, E. R.; Gaunt, A. J.; Hayton, T. W.; May, I.; Reilly, S. D.; Scott, B. L.; Wu, G. *Chem. Commun.* **2011**, *47*, 7647−7649.

(15) Bradley, J. A.; Sen Gupta, S.; Seidler, G. T.; Moore, K. T.; Haverkort, M. W.; Sawatzky, G. A.; Conradson, S. D.; Clark, D. L.; Kozimor, S. A.; Boland, K. S. *Phys. Rev. B* **2010**, *81*, 193104.

(16) Iversen, B. B.; Larsen, F. K.; Pinkerton, A. A.; Martin, A.; Darovsky, A.; Reynolds, P. A. *Inorg. Chem.* **1998**, *37*, 4559−4566.

(17) Beach, D. B.; Bomben, K. D.; Edelstein, N. M.; Eisenberg, D. C.; Jolly, W. L.; Shinomoto, R.; Streitwieser, A. *Inorg. Chem.* **1986**, *25*, 1735−1737.

(18) Kozimor, S. A.; Yang, P.; Batista, E. R.; Boland, K. S.; Burns, C. J.; Christensen, C. N.; Clark, D. L.; Conradson, S. D.; Hay, P. J.; Lezama, J. S.; Martin, R. L.; Schwarz, D. E.; Wilkerson, M. P.; Wolfsberg, L. E. *Inorg. Chem.* **2008**, *47*, 5365−5371.

(19) Brennan, J. G.; Green, J. C.; Redfern, C. M. *J. Am. Chem. Soc.* **1989**, *111*, 2373−2377.

(20) Denecke, M. A.; Rossberg, A.; Panak, P. J.; Weigl, M.; Schimmelpfennig, B.; Geist, A. *Inorg. Chem.* **2005**, *44*, 8418−8425.

(21) Zhurov, V. V.; Zhurova, E. A.; Pinkerton, A. A. *Inorg. Chem.* **2011**, *50*, 6330−6333.

(22) Minasian, S. G.; Krinsky, J. L.; Arnold, J. *Chem.—Eur. J.* **2011**, *17*, 12234−12245.

(23) Liddle, S. T.; McMaster, J.; Mills, D. P.; Blake, A. J.; Jones, C.; Woodul, W. D. *Angew. Chem., Int. Ed.* **2009**, *48*, 1077−1080.

(24) Brennan, J. G.; Stults, S. D.; Andersen, R. A.; Zalkin, A. *Organometallics* **1988**, *7*, 1329−1334.

(25) Mazzanti, M.; Wietzke, R.; Pecaut, J.; Latour, J.-M.; Maldivi, P.; Remy, M. *Inorg. Chem.* **2002**, *41*, 2389−2399.

(26) Wietzke, R.; Mazzanti, M.; Latour, J.-M.; Pecaut, J.; Cordier, P.-Y.; Madic, C. *Inorg. Chem.* **1998**, *37*, 6690−6697.

(27) Karmazin, L.; Mazzanti, M.; Pecaut, J. *Chem. Commun.* **2002**, 654−655.

(28) Liddle, S. T.; Mills, D. P. *Dalton Trans.* **2009**, 5592−5605.

(29) Minasian, S. G.; Krinsky, J. L.; Rinehart, J. D.; Copping, R.; Tyliszczak, T.; Janousch, M.; Shuh, D. K.; Arnold, J. *J. Am. Chem. Soc.* **2009**, *131*, 13767−13783.

(30) Edelstein, N. *Rev. Chim. Miner.* **1977**, *14*, 149−159.

(31) Edelstein, N.; Brown, D.; Whittaker, B. *Inorg. Chem.* **1974**, *13*, 563−567.

(32) Seaman, L. A.; Fortier, S.; Wu, G.; Hayton, T. W. *Inorg. Chem.* **2011**, *50*, 636−646.

(33) Fortier, S.; Wu, G.; Hayton, T. *Inorg. Chem.* **2008**, *47*, 4752−4761.

(34) Fortier, S.; Melot, B. C.; Wu, G.; Hayton, T. W. *J. Am. Chem. Soc.* **2009**, *131*, 15512−15521.

(35) Fortier, S.; Walensky, J. R.; Wu, G.; Hayton, T. W. *J. Am. Chem. Soc.* **2011**, *133*, 11732−11743.

(36) Lewis, R. A.; Wu, G.; Hayton, T. W. *Inorg. Chem.* **2011**, *50*, 4660−4668.

(37) Lewis, R. A.; Wu, G.; Hayton, T. W. *J. Am. Chem. Soc.* **2010**, *132*, 12814−12816.

(38) Bordwell, F. G.; Ji, G. Z. *J. Am. Chem. Soc.* **1991**, *113*, 8398−8401.

(39) Kiplinger, J. L.; Morris, D. E.; Scott, B. L.; Burns, C. J. *Organometallics* **2002**, *21*, 3073−3075.

(40) Ferreira, M. J.; Matos, I.; Ascenso, J. R.; Duarte, M. T.; Marques, M. M.; Wilson, C.; Martins, A. M. *Organometallics* **2007**, *26*, 119−127.

(41) Ferreira, M. J.; Martins, A. M. *Coord. Chem. Rev.* **2006**, *250*, 118−132.

(42) Martins, A. M.; Marques, M. M.; Ascenso, J. R.; Dias, A. R.; Duarte, M. T.; Fernandes, A. C.; Fernandes, S.; Ferreira, M. J.; Matos, I.; Conceição Oliveira, M.; Rodrigues, S. S.; Wilson, C. *J. Organomet. Chem.* **2005**, *690*, 874−884.

(43) Armstrong, D. R.; Barr, D.; Snaith, R.; Clegg, W.; Mulvey, R. E.; Wade, K.; Reed, D. *Dalton Trans.* **1987**, 1071−1081.

(44) Clegg, W.; Snaith, R.; Shearer, H. M. M.; Wade, K.; Whitehead, G. *Dalton Trans.* **1983**, 1309−1317.

(45) Chan, L.-H.; Rochow, E. G. *J. Organomet. Chem.* **1967**, *9*, 231−250.
(46) Love, B. E.; Tsai, L. *Synth. Commun.* **1992**, *22*, 3101−3108.
(47) Schelter, E. J.; Wu, R.; Veauthier, J. M.; Bauer, E. D.; Booth, C. H.; Thomson, R. K.; Graves, C. R.; John, K. D.; Scott, B. L.; Thompson, J. D.; Morris, D. E.; Kiplinger, J. L. *Inorg. Chem.* **2010**, *49*, 1995−2007.
(48) Hilton, D. J.; Prasankumar, R. P.; Schelter, E. J.; Thorsmolle, V. K.; Trugman, S. A.; Schreve, A. P.; Kiplinger, J. L.; Morris, D. E.; Taylor, A. J. *J. Phys. Chem. A* **2008**, *112*, 7840−7847.
(49) Graves, C. R.; Vaughn, A. E.; Schelter, E. J.; Scott, B. L.; Thompson, J. D.; Morris, D. E.; Kiplinger, J. L. *Inorg. Chem.* **2008**, *47*, 11879−11891.
(50) Schelter, E. J.; Yang, P.; Scott, B. L.; Thompson, J. D.; Martin, R. L.; Hay, P. J.; Morris, D. E.; Kiplinger, J. L. *Inorg. Chem.* **2007**, *46*, 7477−7488.
(51) Schelter, E. J.; Yang, P.; Scott, B. L.; Da Re, R. E.; Jantunen, K. C.; Martin, R. L.; Hay, P. J.; Morris, D. E.; Kiplinger, J. L. *J. Am. Chem. Soc.* **2007**, *129*, 5139−5152.
(52) Schelter, E. J.; Veauthier, J. M.; Thompson, J. D.; Scott, B. L.; John, K. D.; Morris, D. E.; Kiplinger, J. L. *J. Am. Chem. Soc.* **2006**, *128*, 2198−2199.
(53) Clark, A. E.; Martin, R. L.; Hay, P. J.; Green, J. C.; Jantunen, K. C.; Kiplinger, J. L. *J. Phys. Chem. A* **2005**, *109*, 5481−5491.
(54) Morris, D. E.; Da Re, R. E.; Jantunen, K. C.; Castro-Rodriguez, I.; Kiplinger, J. L. *Organometallics* **2004**, *23*, 5142−5153.
(55) Jantunen, K. C.; Burns, C. J.; Castro-Rodriguez, I.; Da Re, R. E.; Golden, J. T.; Morris, D. E.; Scott, B. L.; Taw, F. L.; Kiplinger, J. L. *Organometallics* **2004**, *23*, 4682−4692.
(56) Da Re, R. E.; Jantunen, K. C.; Golden, J. T.; Kiplinger, J. L.; Morris, D. E. *J. Am. Chem. Soc.* **2005**, *127*, 682−689.
(57) Schelter, E. J.; Wu, R.; Scott, B. L.; Thompson, J. D.; Morris, D. E.; Kiplinger, J. L. *Angew. Chem., Int. Ed.* **2008**, *47*, 2993−2996.
(58) Diaconescu, P. L.; Cummins, C. C. *J. Am. Chem. Soc.* **2002**, *124*, 7660−7661.
(59) Berthet, J. C.; Ephritikhine, M. *Coord. Chem. Rev.* **1998**, *178*−*180*, 83−116.
(60) Meyer, K.; Mindiola, D. J.; Baker, T. A.; Davis, W. M.; Cummins, C. C. *Angew. Chem., Int. Ed.* **2000**, *39*, 3063−3066.
(61) Fortier, S.; Wu, G.; Hayton, T. W. *Inorg. Chem.* **2009**, *48*, 3000−3011.
(62) Castro-Rodriguez, I.; Olsen, K.; Gantzel, P.; Meyer, K. *J. Am. Chem. Soc.* **2003**, *125*, 4565−4571.
(63) Hutchison, C. A.; Elliot, N. *J. Chem. Phys.* **1948**, *16*, 920−927.
(64) Castro-Rodriguez, I.; Meyer, K. *Chem. Commun.* **2006**, 1353−1368.
(65) Bart, S. C.; Heinemann, F. W.; Anthon, C.; Hauser, C.; Meyer, K. *Inorg. Chem.* **2009**, *48*, 9419−9426.
(66) Schelter, E. J.; Veauthier, J. M.; Graves, C. R.; John, K. D.; Scott, B. L.; Thompson, J. D.; Pool-Davis-Tournear, J. A.; Morris, D. E.; Kiplinger, J. L. *Chem.—Eur. J.* **2008**, *14*, 7782−7790.
(67) Lam, O. P.; Anthon, C.; Heinemann, F. W.; Connor, J. M.; Meyer, K. *J. Am. Chem. Soc.* **2008**, *130*, 6567−6576.
(68) Lam, O. P.; Bart, S. C.; Kameo, H.; Heinemann, F. W.; Meyer, K. *Chem. Commun.* **2010**, *46*, 3137−3139.
(69) Lam, O. P.; Feng, P. L.; Heinemann, F. W.; O'Connor, J. M.; Meyer, K. *J. Am. Chem. Soc.* **2008**, *130*, 2806−2816.
(70) Kozimor, S. A.; Bartlett, B. M.; Rinehart, J. D.; Long, J. R. *J. Am. Chem. Soc.* **2007**, *129*, 10672−10674.
(71) Spencer, L. P.; Schelter, E. J.; Yang, P.; Gdula, R. L.; Scott, B. L.; Thompson, J. D.; Kiplinger, J. L.; Batista, E. R.; Boncella, J. M. *Angew. Chem., Int. Ed.* **2009**, *48*, 3795−3798.
(72) Bart, S. C.; Anthon, C.; Heinemann, F. W.; Bill, E.; Edelstein, N. M.; Meyer, K. *J. Am. Chem. Soc.* **2008**, *130*, 12536−12546.
(73) Graves, C. R.; Yang, P.; Kozimor, S. A.; Vaughn, A. E.; Clark, D. L.; Conradson, S. D.; Schelter, E. J.; Scott, B. L.; Thompson, J. D.; Hay, P. J.; Morris, D. E.; Kiplinger, J. L. *J. Am. Chem. Soc.* **2008**, *130*, 5272−5285.
(74) Castro-Rodriguez, I.; Nakai, H.; Meyer, K. *Angew. Chem., Int. Ed.* **2006**, *45*, 2389−2392.
(75) Burns, G.; Axe, J. D. Covalent Bonding Effects in Rare Earth Crystal Fields. In *Optical Properties of Ions in Crystals*; Crosswhite, H. M., Moos, H. W., Eds.; Interscience: New York, 1967; pp 53−71.
(76) Wybourne, B. G. *Spectroscopic Properties of Rare Earths.*: John Wiley and Sons, Inc.: New York, 1965.
(77) Moritz, A.; Dolg, M. *Chem. Phys.* **2007**, *337*, 48−54.
(78) Chang, A. H. H.; Pitzer, R. M. *J. Am. Chem. Soc.* **1989**, *111*, 2500−2507.
(79) Gaunt, A. J.; Reilly, S. D.; Enriquez, A. E.; Scott, B. L.; Ibers, J. A.; Sekar, P.; Ingram, K. I. M.; Kaltsoyannis, N.; Neu, M. P. *Inorg. Chem.* **2008**, *47*, 29−41.
(80) Strittmatter, R. J.; Bursten, B. E. *J. Am. Chem. Soc.* **1991**, *113*, 552−559.
(81) Kiplinger, J. L.; Morris, D. E.; Scott, B. L.; Burns, C. J. *Organometallics* **2002**, *21*, 5978−5982.
(82) Jennings, J. R.; Snaith, R.; Mahmoud, M. M.; Wallwork, S. C.; Bryan, S. J.; Halfpenny, J.; Petch, E. A.; Wade, K. *J. Organomet. Chem.* **1983**, *249*, c1−c5.
(83) Barr, D.; Clegg, W.; Mulvey, R. E.; Snaith, R.; Wade, K. *J. Chem. Soc., Chem. Commun.* **1986**, 295−297.
(84) Bain, G. A.; Berry, J. F. *J. Chem. Educ.* **2008**, *85*, 532.
(85) Piehler, D.; Kot, W. K.; Edelstein, N. *J. Chem. Phys.* **1991**, *94*, 942.
(86) Görller-Walrand, C.; Binnemans, K. In *Handbook on the Physics and Chemistry of Rare Earths*; Gschneider, K. A., Eyring, L., Eds.; Elsevier Science B.V.: Amsterdam, 1967; Vol. *23*, pp 121−283.
(87) Gamp, E.; Edelstein, N.; Malek, C. K.; Hubert, S.; Genet, M. *J. Chem. Phys.* **1983**, *79*, 2023.
(88) *SMART Software Users Guide*; Bruker Analytical X-Ray Systems, Inc.: Madison, WI, 1999; Vol. Version 5.1.
(89) *SAINT Software Users Guide*; Bruker Analytical X-Ray Systems, Inc.: Madison, WI, 1999; Vol. Version 5.1.
(90) Sheldrick, G. M. *SADABS*; University of Gottingen, Germany, 2005.
(91) Sheldrick, G. M. *SHELXTL*; Bruker Analytical X-Ray Systems, Inc.: Madison, WI, 2001; Vol. *6.12*.